

A THEORETICAL STUDY OF MAGNETIC  
SELF-PINCHING IN A SEMICONDUCTOR

by

WILLIAM MURRAY STROME  
B.Sc., University of Alberta, 1960

A THESIS SUBMITTED IN PARTIAL FULFILMENT OF  
THE REQUIREMENTS FOR THE DEGREE OF  
MASTER OF APPLIED SCIENCE

in the Department  
of  
PHYSICS

We accept this thesis as conforming to the  
required standard

THE UNIVERSITY OF BRITISH COLUMBIA

January, 1962

In presenting this thesis in partial fulfilment of the requirements for an advanced degree at the University of British Columbia, I agree that the Library shall make it freely available for reference and study. I further agree that permission for extensive copying of this thesis for scholarly purposes may be granted by the Head of my Department or by his representatives. It is understood that copying or publication of this thesis for financial gain shall not be allowed without my written permission.

Department of Physics

The University of British Columbia,  
Vancouver 8, Canada.

Date January 31, 1962

## ABSTRACT

The subject of this thesis is the theoretical investigation of the possibility of observing magnetic self-pinching of the hole-electron plasma present in a semiconductor. The steady-state pinch equations are derived for conditions which might be expected to prevail in such a plasma, both with and without the effects of generation and recombination.

Recent reports of the observance of pinch effect in indium antimonide operated under avalanche breakdown conditions are discussed. All these reports based their claim of observing pinch on slight changes in overall resistance of the sample, a purely secondary effect of self-pinching. It is indicated that a plasma generated by avalanching is a poor medium from which to compare experimental results with available theory. Hence it is concluded that the above reports offer only circumstantial evidence of self-pinching.

Finally, an experimental arrangement is suggested with which one should be able to determine unambiguously whether or not pinch can occur in semiconductors.

TABLE OF CONTENTS

	Page
1. INTRODUCTION	1
2. PINCH EQUATIONS	
2.1 Model	3
2.2 Cylindrical Geometry	6
2.3 Slab Geometry	8
2.4 Comparison Between the Cylinder and the Slab	11
2.5 Estimation of Pinch Time in Cylindrical Plasma	11
5. GENERATION AND RECOMBINATION	
3.1 Statement of the Problem	14
3.2 Development of the Equations	14
3.3 Conditions whereby G & R may be Neglected	17
3.4 Numerical Solution	18
3.5 Surface Recombination	19
3.6 Recombination Time	20
4. THERMAL EFFECTS	
4.1 Assumptions	22
4.2 Cylindrical Geometry	23
4.3 Slab Geometry	24
4.4 Comparison of the Two Geometries	26

	Page
5. PUBLISHED EXPERIMENTAL DATA	
5.1 General Review	28
5.2 Critical Summary	31
6. EXPERIMENTAL CONSIDERATIONS	
6.1 Observable Characteristic of Pinch	35
6.2 Radio-Frequency Measurements	36
6.3 Probe Techniques	38
6.4 Infrared Absorption	38
6.5 Generation of a Hole-Electron Plasma	40
6.6 Geometry and Material	41
6.7 Summary	46
7. CONCLUSIONS	47
APPENDIX	
Some Properties of Three Intrinsic Semiconducting Materials	49
BIBLIOGRAPHY	52
LIST OF FIGURES	
2-1. Orientation of coordinate system with respect to sample	9
3-1. Carrier distribution for $\Gamma=0.5$ ; various values of $w/L_D$ .	(to follow page 19)-1
3-2. Carrier distribution for $\Gamma=1.5$ ; various values of $w/L_D$ .	(to follow page 19)-2
3-3. Carrier distribution for $\Gamma=5.0$ ; various values of $w/L_D$ .	(to follow page 19)-3
3-4a. Average absolute deviation of $\eta$ from unity as a function of $w/L_D$ ; for three values of $\Gamma$ .	(to follow page 19)-4

LIST OF FIGURES (continued)

Page

3-4b. Normalised average absolute deviation of  $\eta$  from unity as a function of  $w\lambda_{D_i}$  for three values of  $r$ .

(to follow page 19)-4

6-1. Experimental arrangement for measuring the carrier distribution by infrared absorption.

39

## ACKNOWLEDGEMENTS

I should like to express my gratitude to Professor R. E. Burgess, my thesis supervisor, for his invaluable guidance and assistance during the preparation of this work.

I am also indebted to the National Research Council of Canada for the financial assistance given me through a Bursary and a Studentship.

## 1. INTRODUCTION

For a number of years, self-pinching (or magnetic self-focusing) of the current carriers in a gaseous plasma has been discussed in the literature. During the past few years some interest has arisen in the possibility of observing a similar effect in the hole-electron plasma present in a semiconductor. This thesis is concerned with a theoretical investigation of this possibility.

In chapters 2 and 3 we develop the theory of steady-state magnetic pinch. We first neglect the effects of generation and recombination (G & R) to develop the pinch equations for a bounded plasma under conditions expected in a semiconductor. This analysis leads to results similar to those originally derived by Bennett (1934) for an unbounded gaseous plasma. We consider two sample geometries: slab and cylindrical. We also give an estimate of the time required for pinch to develop. We then consider the effects of G & R in the slab geometry.

The results of numerical solution of the resulting differential equation show that G & R has a strong inhibitory effect on the pinch, as would be expected.

In any pinch experiment one must be careful to eliminate, or at least account for thermal effects. Thus chapter 4 is devoted to the investigation of these effects in

slab and cylindrical shaped semiconductor samples.

Very recently, a number of workers (Glicksman and Steele, 1959; Glicksman and Powlus, 1961; Ancker-Johnson et al, 1961; and Chynoweth and Murray, 1961) have reported observations of phenomena in indium antimonide operated under avalanche conditions which they have ascribed to pinch. Their measurements involved slight changes in the resistance of the sample during "pinch". In chapter 5 we discuss the results of the above-mentioned workers and point out that their evidence for pinch is only circumstantial, and that avalanching is a poor method of producing a plasma for rigorous comparison of pinch theory to experimental results.

Finally, chapter 6 is devoted to investigation of possible methods of determining unambiguously whether or not pinch occurs in a semiconductor. From all considerations we show that pinch should be detectable by probe measurements of the conductivity distribution in a pure germanium slab at about room temperature.

## 2. PINCH EQUATIONS

### 2.1 Model

For the starting point in the theoretical discussion of pinch effect in semiconductors we take a rather simplified model. We assume that  $n=p=n_i$  in the undisturbed state where  $n$  and  $p$  are the electron and hole concentrations respectively, and  $n_i$  is the initial carrier concentration. Initially we will consider only a distribution of the carriers which is in dynamic equilibrium without any regard as to how this distribution arises, or to its stability. (Later we will try to estimate the time required for pinch to develop.)

It will be assumed that the carrier mobilities ( $\mu_p$  and  $\mu_n$  for holes and electrons, respectively) and the diffusion coefficients ( $D_p$  and  $D_n$  for holes and electrons) are constants independent of the carrier concentration. Neglecting generation and recombination of hole-electron pairs, there will be no net carrier velocity in the transverse (or radial) directions.

Although initially the hole and electron concentrations are both equal to the initial carrier concentration, we admit the possibility that under pinch conditions, the local hole and electron concentrations may differ from each other slightly.

There are a number of ways in which the "steady-

state" pinch equations may be obtained. Bennett (1934) originally obtained one form of these equations by considering the relativistic inter-particle forces in two oppositely directed streams of oppositely charged particles.

In this section, we shall derive the pinch equations through:

$$\left. \begin{aligned} \bar{J}_n &= q \mu_n \{ n (\bar{E} + \bar{v}_n \times \bar{B}) + (D_n/\mu_n) \nabla n \} \\ \bar{J}_p &= q \mu_p \{ p (\bar{E} + \bar{v}_p \times \bar{B}) - (D_p/\mu_p) \nabla p \} \end{aligned} \right\} \quad (2-1)$$

where  $\bar{J}_p, \bar{J}_n$  are the hole and electron current densities

$\bar{v}_p, \bar{v}_n$  are the hole and electron velocities

$-q$  is the electronic charge

$\bar{B}$  is the magnetic field

and  $\bar{E}$  is the electric field.

We obtain the pinch relations by assuming that the net transverse (or radial) components (denoted by the subscript  $\perp$  in the general case) of current density due to each type of carrier vanishes:

$$J_{n\perp} = J_{p\perp} = 0$$

we form the combination of these vanishing current densities:

$$\mu_p J_{n\perp} - \mu_n J_{p\perp}$$

and then from (2-1) we get

$$(n-p)\bar{E}_\perp + [(n\bar{v}_n - p\bar{v}_p) \times \bar{B}]_\perp + \nabla_\perp \left( \frac{D_n}{\mu_n} n + \frac{D_p}{\mu_p} p \right) = 0 \quad (2-2)$$

Now it can be shown that under pinch conditions,  $E_{\perp}$ ,  $(\vec{v}_n \times \vec{B})_{\perp}$  and  $(D_{\beta}/\mu_{\beta}) \nabla_{\perp} \beta$  (where  $\beta$  may be read as either  $n$  or  $p$ ) are all of the same order of magnitude. Since  $\vec{v}_n$  and  $\vec{v}_p$  are oppositely directed, then provided  $|n-p| \ll n+p$  (i.e.  $n \approx p$ ) we may neglect the first term of (2-2). Approximately:

$$n [ (\vec{v}_n - \vec{v}_p) \times \vec{B} ]_{\perp} + \left( \frac{D_n}{\mu_n} + \frac{D_p}{\mu_p} \right) \nabla_{\perp} n = 0 \quad (2-3)$$

It is customary to introduce the Einstein relation at this point

$$D_{\beta} = k T_{\beta} \mu_{\beta} / q \quad (2-4)$$

to define  $T_{\beta}$  the hole or electron "temperature". This relation is rigorous when the carrier distributions are Maxwellian. It must be used with caution under high field conditions where these distributions may be far from Maxwellian, and the "carrier temperatures" may be quite different from the lattice temperature, and from each other. The "carrier temperature" will be considered that appropriate to a two dimensional velocity distribution (assumed to be approximately Maxwellian) in the plane perpendicular to the drift velocity. In a more exact analysis, the carrier mobilities and the diffusion coefficients would likely be both field and carrier concentration dependent.

Substituting (2-4) into (2-3) we arrive at

$$q n [ (\vec{v}_n - \vec{v}_p) \times \vec{B} ]_{\perp} + k (T_n + T_p) \nabla_{\perp} n = 0 \quad (2-5)$$

which we use together with the Maxwell relation:

$$\nabla \times \vec{B} = \mu (\vec{J}_n + \vec{J}_p) \approx \mu q n (\vec{v}_p - \vec{v}_n) \quad (2-6)$$

(where  $\mu$  is the permeability of the sample) to obtain the pinch equations for the two geometries (cylindrical and slab) in which we are interested. We use the auxiliary condition that carriers are conserved under pinch, i.e. that  $\int_{\text{cross section}} n \, dS = \text{const.}$

## 2.2 Cylindrical Geometry

By assuming cylindrical geometry we obtain the following differential equation for the carrier distribution from equations (2-5) and (2-6).

$$\frac{1}{r} \frac{\partial}{\partial r} \left( \frac{r}{n} \frac{\partial n}{\partial r} \right) + \frac{\mu q^2 (v_n + v_p)^2}{k(T_n + T_p)} n = 0 \quad (2-7)$$

(where  $v_n$  and  $v_p$  are the magnitudes of the respective carrier drift velocities). A solution of this equation is:

$$n(r) = n_0 (1 + br^2)^{-2} \quad (2-8)$$

where

$$b = n_0 \cdot \mu q^2 (v_n + v_p)^2 / 8k(T_n + T_p) \quad (2-9)$$

and  $n_0$ , the carrier density along the axis is found by invoking conservation of carriers:

$$\pi a^2 n_i = \int_0^a n(r) 2\pi r \, dr$$

where  $a$  is the radius of the sample. This yields

$$n_0 = n_i \left\{ 1 - \frac{\mu I^2}{8\pi N k (T_n + T_p)} \right\}^{-1} \quad (2-10)$$

where  $N = \pi a^2 n_i$ , the number of carriers of one kind per unit length.

In Bennett's (1934) original development of the pinch equations, he considered only the case of an unbounded plasma. In this situation, one can obtain a critical current,  $I'_{CR}$ , which is necessary to maintain the distribution given by (2-8) appropriate to an unbounded plasma for which  $n_0$  and  $b$  are undetermined.

$$I'_{CR} = [8\pi Nk(T_n + T_p)/\mu]^{1/2} \quad (2-11)$$

The criterion for self-pinching most often quoted in the literature is that the current,  $I$ , must exceed the value of  $I'_{CR}$  given in (2-11). However if we substitute this value into (2-10) we obtain an infinite value of  $n_0$  indicating that all of the carriers are concentrated on the axis at that current. Since this cannot happen physically, our solution must break down as  $I \rightarrow I'_{CR}$ .

For the purpose of our investigation, let us define arbitrarily a critical current,  $I_{CR}$ , as one which will reduce the number of carriers at the outer surface to one half the initial value,  $n_i$ , (or double the concentration on the axis). Putting  $r = a$  in (2-8) and substituting the values of  $n_0$  and  $b$  from (2-9) and (2-10) we find that from the above definition,

$$I_{CR} = [4\pi Nk(T_n + T_p)/\mu]^{1/2} \quad (2-12)$$

If we define  $\gamma = (I/I_{CR})^2$ , a measure of the strength of the pinch, we may write some of the previous results in terms of it: (over)

$$n(r) = n_i (1 - r/2) \left[ 1 - \frac{1}{2} r \left\{ 1 - (r/a)^2 \right\} \right]^{-2}$$

$$b = \frac{1}{2} r \left[ a^2 (1 - \frac{1}{2} r) \right]^{-1}$$

$$n_o = n_i \left[ 1 - \frac{1}{2} r \right]^{-1}$$

$$B_\phi = \frac{\mu I}{2\pi a} \cdot \frac{r/a}{\left[ 1 - \frac{1}{2} r \left\{ 1 - (r/a)^2 \right\} \right]}$$

Since carriers are conserved and we assume the mobilities to remain constant, the resistance of the sample is given by

$$R = \ell / N q (\mu_n + \mu_p) \quad (2-13)$$

where  $\ell$  is the length of the sample. From (2-12) and (2-13) we obtain expressions for the longitudinal electric field and the power dissipation in the sample:

$$\left. \begin{aligned} E_{\text{long.}} &= \left[ \frac{4\pi k (T_n + T_p)}{\mu q^2 N (\mu_n + \mu_p)^2} r \right]^{1/2} \\ P &= \frac{4\pi k (T_n + T_p)}{\mu q (\mu_n + \mu_p)} \ell r \end{aligned} \right\} \quad (2-14)$$

### 2.3 Slab Geometry

We will choose a coordinate system oriented as shown in Figure 2-1 with respect to the sample. (Over)

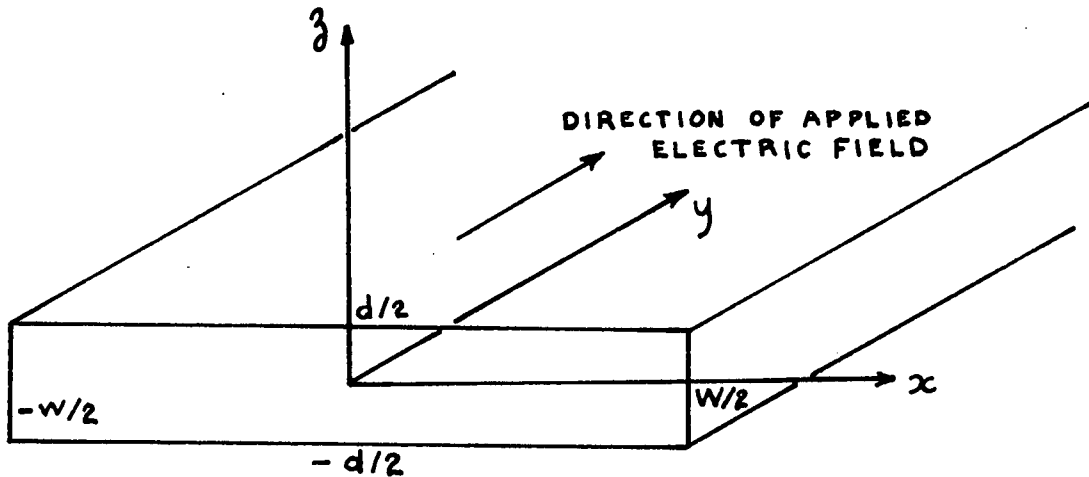


Figure 2-1. Orientation of coordinate system with respect to sample.

If we assume that the thickness  $d$  is much less than the width  $w$ , and that transverse components of current density vanish as before, we need only consider the  $x$ -components of the terms in equations (2-5) and (2-6) since the  $z$ -components will give a negligible contribution to the pinch. (Note that this is true only as long as the majority of the carriers are outside the region bounded by  $x = \pm d/2$ .) As in section 2.2, we can obtain a differential equation for the carrier distribution:

$$\frac{\partial}{\partial x} \left( \frac{1}{n} \cdot \frac{\partial n}{\partial x} \right) + \frac{\mu q^2 (v_n + v_p)^2}{k(T_n + T_p)} n = 0 \quad (2-15)$$

The solution of (2-15) is of the form

$$n(x) = n_0 \operatorname{sech}^2(\sqrt{b'} x) \quad (2-16)$$

where 
$$n_0 = b' \left[ 2k(T_n + T_p) / \mu q^2 (\nu_n + \nu_p)^2 \right] \quad (2-17)$$

and  $b'$  is obtained from the conservation of carriers:

$$n_i w d = 2d \int_0^{w/2} n(x) dx$$

which leads to the following transcendental equation in  $b'$ :

$$\sqrt{b'} (w/2) \tanh(\sqrt{b'} w/2) = \left(\frac{w}{d}\right) \cdot \left[ \mu I^2 / 8Nk(T_n + T_p) \right] \quad (2-18)$$

If we define the critical current as in section 2.2, i.e. that at which  $n(\pm w/2) = n_i/2$ , then we find that

$$I_{CR} = \left[ 8(d/w)Nk(T_n + T_p) / \mu \right]^{1/2} \quad (2-19)$$

We can also find the current at which our analysis begins to break down — that at which about half of the carriers are within the region bounded by  $x = \pm d/2$ . This is at a current approximately equal to  $[0.55w/d]^{1/2} I_{CR}$ .

As in section 2.2, with the resistance of the sample as given by (2-13), we can obtain the electric field and power dissipation in the sample:

$$E_{\text{long.}} = \left[ \frac{8(d/w)k(T_n + T_p)}{\mu q^2 N (\mu_n + \mu_p)^2} \right]^{1/2} \cdot \Gamma^{1/2}$$

$$P = \frac{8(d/w)k(T_n + T_p)}{\mu q (\mu_n + \mu_p)} l \cdot \Gamma \quad (2-20)$$

where

$$\Gamma = (I / I_{CR})^2.$$

## 2.4 Comparison Between the Cylinder and the Slab

Let us compare the current, electric field, and power dissipation required to initiate pinching (by our arbitrary definition of the onset of pinch —  $n(\text{edge}) = \frac{n_i}{2}$ ). It is assumed that samples of the same material with the same physical properties and of the same length and cross-sectional area are to be compared. At  $I = I_{CR}$  :

$$\left. \begin{aligned} I_{CR}(\text{slab}) / I_{CR}(\text{cyl.}) &= (2d / \pi w)^{1/2} \\ E_{CR}(\text{slab}) / E_{CR}(\text{cyl.}) &= (2d / \pi w)^{1/2} \\ P_{CR}(\text{slab}) / P_{CR}(\text{cyl.}) &= 2d / \pi w \end{aligned} \right\} \quad (2-21)$$

Since  $d/w$  is assumed to be much less than unity, the current, electric field, and power dissipation can all be lower in the case of the slab geometry.

## 2.5 Estimation of Pinch Time in Cylindrical Plasma

In the case of the cylinder, considering only the radial components, equations (2-1) with (2-4) may be written

$$\left. \begin{aligned} J_{nr} &= q \mu_n \left[ n (E_r + v_n B_\phi) + \frac{k T_n}{q} \cdot \frac{\partial n}{\partial r} \right] \\ J_{pr} &= q \mu_p \left[ p (E_r - v_p B_\phi) - \frac{k T_p}{q} \cdot \frac{\partial p}{\partial r} \right] \end{aligned} \right\} \quad (2-22)$$

The continuity equations are

$$\nabla \cdot \vec{J}_n = q \frac{\partial n}{\partial t} \quad (2-23)$$

$$\nabla \cdot \vec{J}_p = -q \frac{\partial p}{\partial t}$$

Let us define a new current density

$$J_r' = \frac{\mu_n}{\mu_n + \mu_p} \cdot J_{pr} - \frac{\mu_p}{\mu_n + \mu_p} \cdot J_{nr} \quad (2-24)$$

Our reason for this particular combination of  $J_n$  and  $J_p$  is that if, as usual,  $|n-p| \ll n+p$  (i.e.  $n \approx p$ ), approximately:

$$\nabla_r \cdot \vec{J}' = \frac{1}{r} \frac{\partial}{\partial r} (r J_r') = -q \frac{\partial n}{\partial t} \quad (2-25)$$

The only component of  $\vec{J}'$  of interest is the radial one. From (2-22) and (2-24)

$$J_r' = -q \frac{\mu_n \mu_p}{\mu_n + \mu_p} \left\{ n (v_n + v_p) B_\phi + \frac{k(T_n + T_p)}{q} \cdot \frac{\partial n}{\partial r} \right\} \quad (2-26)$$

Let us now define

$$g = \int_0^a n(r) r^3 dr \quad (2-27)$$

which is proportional to the number moment of inertia of the hole-electron plasma. So long as  $\partial g / \partial t$  is negative the plasma is contracting. From (2-25), (2-27) and the condition that carriers are conserved at all times which leads to

$$J_r'(a) = 0 \quad \text{we get:}$$

$$\frac{\partial g}{\partial t} = \frac{2}{q} \int_0^a J_r' r^2 dr$$

which becomes, from (2-6) and (2-26)

$$\frac{\partial g}{\partial t} = -\frac{\mu_n \mu_p}{\mu_n + \mu_p} \cdot \frac{2Nk(T_n + T_p)}{\pi q} \left\{ \frac{MI^2}{8\pi Nk(T_n + T_p)} - \left(1 - \frac{n(a)}{n_i}\right) \right\} \quad (2-28)$$

Notice that when  $\partial g / \partial t = 0$ ,  $n(a)$  is given by

$$\frac{n(a)}{n_i} = 1 - \frac{1}{2} (I/I_{CR})^2 \quad (2-29)$$

where  $I_{CR}$  is defined in equation (2-12), which is the same as the expression given by the steady state analysis. Thus, let us suppose that the carrier concentration at the outer edge approaches the value given by (2-29) exponentially from  $n_i$ , the value before pinching commences, i.e. assume

$$n(a)(t) = n_i \left\{ e^{-t/\tau_p} + \left[1 - \frac{1}{2} (I/I_{CR})^2\right] \cdot [1 - e^{-t/\tau_p}] \right\}$$

where  $\tau_p$  is the "pinching time constant" to be determined.

Substituting the above into 2-28)

$$\frac{\partial g}{\partial t} = -\frac{\mu_n \mu_p}{\mu_n + \mu_p} \cdot \frac{Nk(T_n + T_p)}{\pi q} (I/I_{CR})^2 e^{-t/\tau_p} \quad (2-30)$$

Using the definition of  $g$  given by equation (2-27), the initial carrier distribution ( $n \equiv n_i$ ) and the final steady state distribution (at  $t = \infty$ ) given by equation (2-8) in one form, we can obtain an expression for  $\tau_p$ :

$$\tau_p = \frac{\left[ \frac{2}{\gamma} \left( 1 - 2 \frac{(1 - \frac{1}{2}\gamma)}{(\frac{1}{2}\gamma)^2} \left\{ \ln \left( \frac{1}{1 - \frac{1}{2}\gamma} \right) - \frac{1}{2}\gamma \right\} \right) \right]}{8 \left( \frac{\mu_n \mu_p}{\mu_n + \mu_p} \right) k (T_n + T_p)} a^2 q \quad (2-31)$$

where for compactness we have put  $(I/I_{cr})^2 = \gamma$ .

The portion of (2-31) in the square bracket is a rather weak increasing function of  $\gamma$  ranging from 1/3 at  $\gamma=0$  to unity at  $\gamma=2$ .

### 3. GENERATION AND RECOMBINATION

#### 3.1 Statement of the Problem

To this time we have not considered the effect generation and recombination (henceforth abbreviated G & R) will have upon the pinch distribution. This effect has also apparently been overlooked in the literature — probably because the effect is negligible in a gaseous plasma, and most of the work concerned with pinch in semiconductors is a direct adaptation of the gaseous theory.

In an intrinsic semiconductor under low field conditions, virtually all the carriers present result from thermal generation balanced against recombination. Hence, qualitatively, one can see that any effort to disturb the local concentration of the carriers will be strongly opposed by thermal G & R.

#### 3.2 Development of the Equations

We will concern ourselves in this discussion only with the case of slab geometry. The coordinate axes will again be oriented as shown in Figure 2-1. If we define  $\vec{J}'$  as in

equation (2-24) we may combine equations (2-1) to get (taking only the  $x$ -component since we are again assuming  $d/w \ll 1$ ):

$$J'_x = q \frac{\mu_n \mu_p}{\mu_n + \mu_p} \left\{ n (v_n + v_p) B_3 - \frac{k(T_n + T_p)}{q} \frac{\partial n}{\partial x} \right\} \quad (3-1)$$

At this point we do not set  $J_{n_x} = J_{p_x} = 0$  as in the previous chapter. Instead, we make use of the steady-state continuity equation:

$$\nabla \cdot \bar{J}_p = -\nabla \cdot \bar{J}_n = q(g - \mathcal{R})$$

where  $g$  and  $\mathcal{R}$  are the pair generation and recombination rates respectively.

Since  $n \approx p$ , as usual, we may write to a good approximation (Smith, 1959, p. 252):

$$\nabla \cdot \bar{J}_p = -\nabla \cdot \bar{J}_n = q \mathcal{R}_0 [1 - (n/n_i)^2]$$

or from the definition of  $\bar{J}'$ ,

$$\frac{\partial J'_x}{\partial x} = q \mathcal{R}_0 [1 - (n/n_i)^2] \quad (3-2)$$

where  $\mathcal{R}_0$  is the thermal generation rate per unit volume.

Usually at this point in any analysis involving G & R, it is assumed that  $(n - n_i) \ll n_i$ , in which case (3-2) may be linearized so that  $[1 - (n/n_i)^2]$  becomes approximately  $2[1 - n/n_i]$ . However doing this in our case does not appreciably simplify the final equation.

From equations (2- 6), (3- 1) and (3- 2)

$$\frac{\partial}{\partial x} \left\{ \frac{1}{n} \left( \frac{\partial n}{\partial x} + \frac{(\mu_n + \mu_p) q R_o}{\mu_n \mu_p k (T_n + T_p)} \int_0^x [1 - (n/n_i)^2] dx \right) + n \frac{\mu q^2 (v_n + v_p)^2}{k (T_n + T_p)} \right\} = 0 \quad (3- 3)$$

It was not possible to find an analytical solution to the above equation. Thus, the equation was put into a form more amenable to numerical solution by means of the following substitutions:

$$\left. \begin{aligned} \xi &= 2x/w \\ \eta &= n/n_i \\ \Gamma &= \mu q^2 (v_n + v_p)^2 n_i w^2 / 8k (T_n + T_p) = (I/I_{ca})^2 \\ L_{0i}^2 &= \frac{\mu_n \mu_p}{\mu_n + \mu_p} \cdot \frac{k (T_n + T_p)}{4q R_o} n_i \end{aligned} \right\} \quad (3- 4)$$

is a form of ambipolar diffusion length in the undisturbed sample. If  $n=p=n_i$ , the ambipolar diffusion length is given by

$$L^2 = \frac{n_i k}{2 R_o} \left( \frac{1}{\mu_n T_n} + \frac{1}{\mu_p T_p} \right)^{-1} = \frac{1}{\tau_i} \cdot \frac{D_n D_p}{D_n + D_p}$$

where  $\tau_i$  is the carrier lifetime. This is the same as our  $L_{0i}^2$ ; in the special case where  $T_n = T_p$ . Making the above substitutions into (3- 3) it becomes

$$\frac{\partial}{\partial \xi} \left\{ \frac{1}{\eta} \left[ \frac{\partial \eta}{\partial \xi} + \frac{1}{16} \left( \frac{w}{L_{0i}} \right)^2 \int_0^{\xi} (1 - \eta^2) d\xi \right] \right\} + 2\Gamma\eta = 0 \quad (3-5)$$

### 3.3 Conditions whereby G & R may be Neglected

Before considering the results of a numerical solution of (3-5), we should look at the conditions under which the effects of G & R may be considered negligible. The condition required is simply:

$$\left| \frac{1}{16} \frac{w}{L_{0i}^2} \int_0^{\xi} (1 - \eta^2) d\xi \right| \ll \left| \frac{\partial \eta}{\partial \xi} \right| \quad (3-6)$$

for  $0 \leq \xi \leq 1$ .

If we assume that (3-6) holds, (3-5) becomes

$$\frac{\partial}{\partial \xi} \left( \frac{1}{\eta} \cdot \frac{\partial \eta}{\partial \xi} \right) + 2\Gamma\eta = 0$$

whose solution is

$$\eta = \frac{b^2}{\Gamma} \operatorname{sech}^2(b\xi)$$

where  $b$  must be determined by boundary conditions. In this discussion we neglect the effects of surface recombination at the outer edge of the sample, and hence an appropriate boundary condition to apply is that the hole and electron current densities vanish at  $x = \pm w/2$ . This condition leads to the following transcendental equation in  $b$

$$\frac{b^3}{\Gamma^2} \tanh(b) \cdot \frac{(1 + \frac{2}{3} \sinh^2(b))}{\cosh^2(b)} = 1 \quad (3-7)$$

Condition (3- 6) may now be written

$$w/L_{D_i} \ll 4 \left\{ \frac{\frac{2b^3}{\Gamma} \operatorname{sech}^2(b\xi) \tanh(b\xi)}{\frac{b^3}{\Gamma^2} \tanh(b\xi) \operatorname{sech}^2(b\xi) (1 + \frac{2}{3} \sinh^2(b\xi)) - \xi} \right\}^{1/2} \quad (3- 8)$$

for all  $\xi$  in the range of interest.

The right-hand expression of (3- 8) has a minimum at  $\xi = 0$  and hence we can obtain the following limit on the ratio  $w/L_{D_i}$  :

$$w/L_{D_i} \ll 4 \left\{ \frac{(2b^4/\Gamma)}{(b^4/\Gamma^2) - 1} \right\}^{1/2} \quad (3- 9)$$

or approximately

$$w/L_{D_i} \ll \sim 4(3 + 2\Gamma)^{1/2} \quad (3-10)$$

It is not the purpose of this section to consider the practical implications of these results; however, we will note that they would be very difficult to satisfy with most available semiconductors.

#### 3.4 Numerical Solution

Equation (3- 5) was solved numerically with the aid of the Alvac III-E digital computer for the values of  $\Gamma = 0.5, 1.5$  and  $5.0$  and values of  $(w/L_{D_i}) = 1, 5, 10, 20$  and  $30$ . While it would have been desirable to take more values of these parameters, the calculations required a considerable amount of time. Also as these parameters became larger, the machine could no longer handle the large range of numbers which arose in the intermediate stages of the calculation.

The results of the numerical calculations are plotted in Figures 3-1, 3-2 and 3-3, where  $\eta$  is plotted against  $\xi$  for various  $\Gamma$  and  $w/L_p$ . The inhibitory effect of the G & R is immediately obvious in all cases.

In Figure 3-4a we have plotted  $D$  against  $w/L_p$  for the three values of  $\Gamma$ . This  $D$  is defined as follows

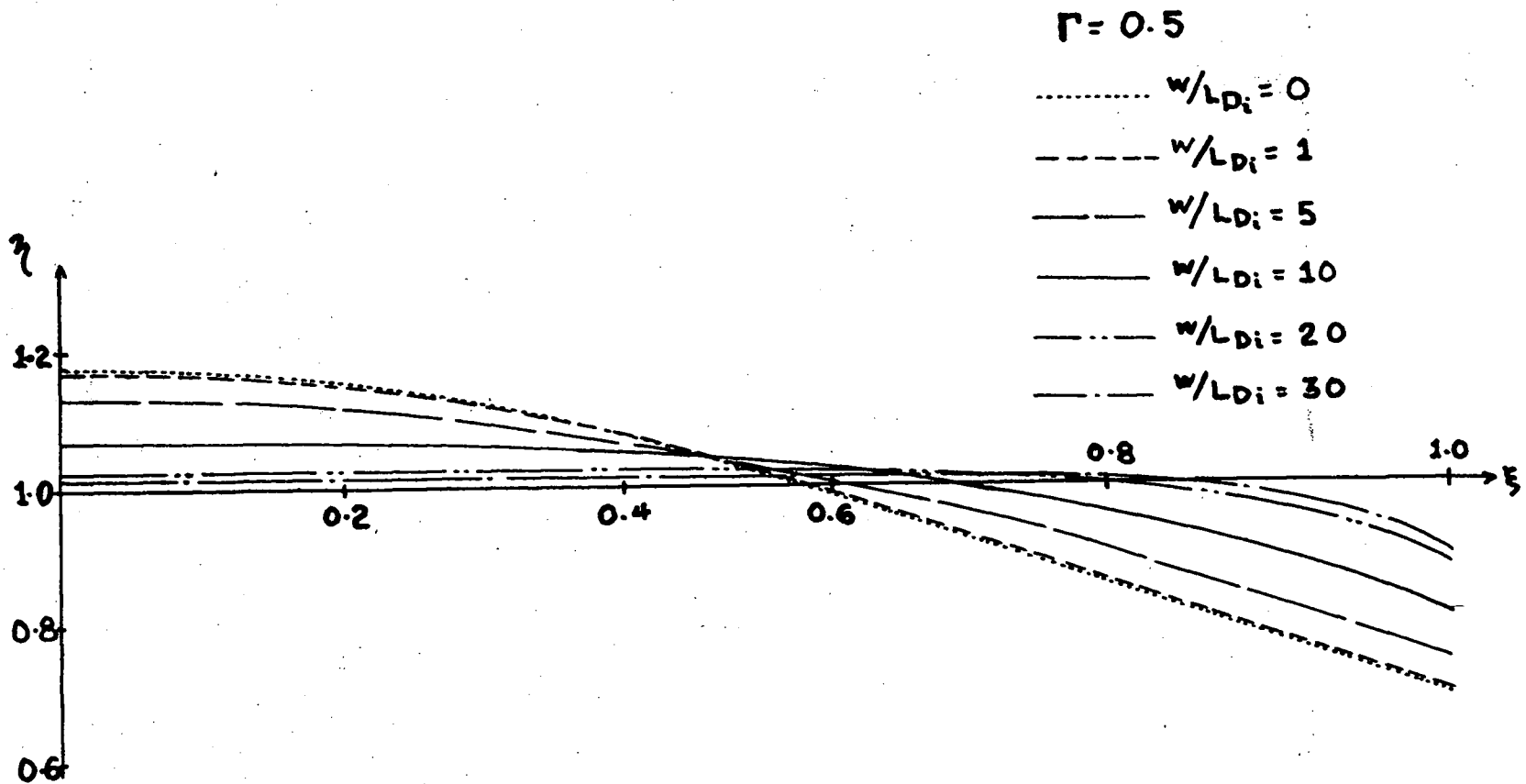
$$D = \frac{1}{17} \sum_{i=0}^{16} \left| \eta(\xi = i/16) - 1 \right| \quad (3-11)$$

We will use this as a measure of the strength of the pinch since it is the deviation of the curve of  $\eta$  vs  $\xi$  from the curve which would result in the unpinched condition, namely  $\eta \equiv 1$ . In Figure 3-4b we have normalized the curves of 4-32. Here we see that the relative inhibition of the pinch is, initially at any rate, a weakly decreasing function of  $\frac{w}{L_p}$ , as would be expected from (3-10).

### 3.5 Surface Recombination

We have considered only recombination within the body of our semiconductor to this point. However, in thin samples the recombination rate at the surface is generally much higher than that in the body of the material. Smith (1959, p. 297 ff.) shows that to a good approximation the rate at which hole electron pairs recombine at the surface, per unit area,  $S_a$  is given by

$$S_a = B_s n_i^2 \left[ (n/n_i)^2 - 1 \right] \quad (3-12)$$



(to follow page 19)-1

Figure 3-1. Carrier distribution for  $\Gamma = 0.5$ ; various values of  $w/L_{Di}$ .

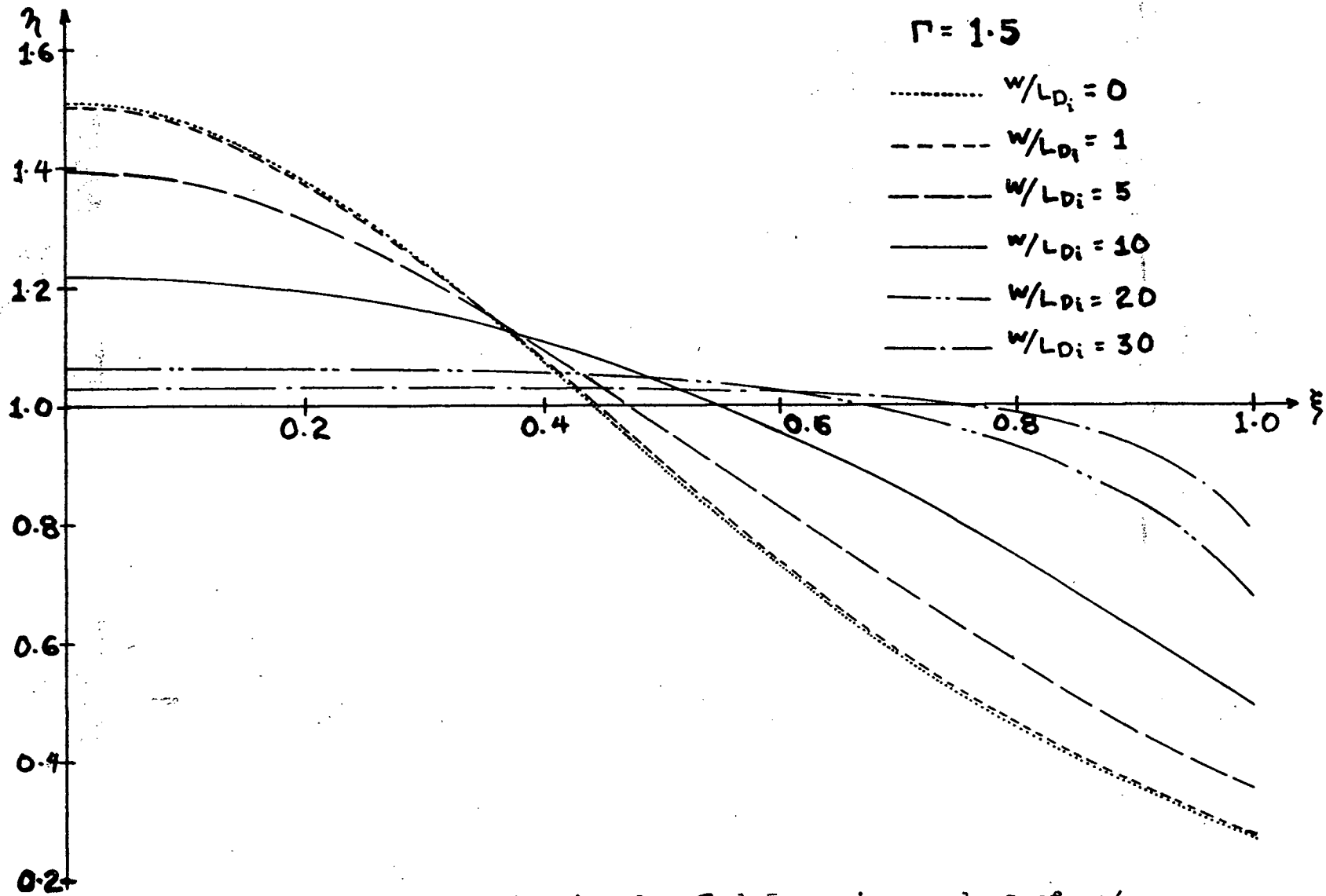


Figure 3-2. Carrier distribution for  $\Gamma = 1.5$ ; various values of  $w/L_{Di}$ .

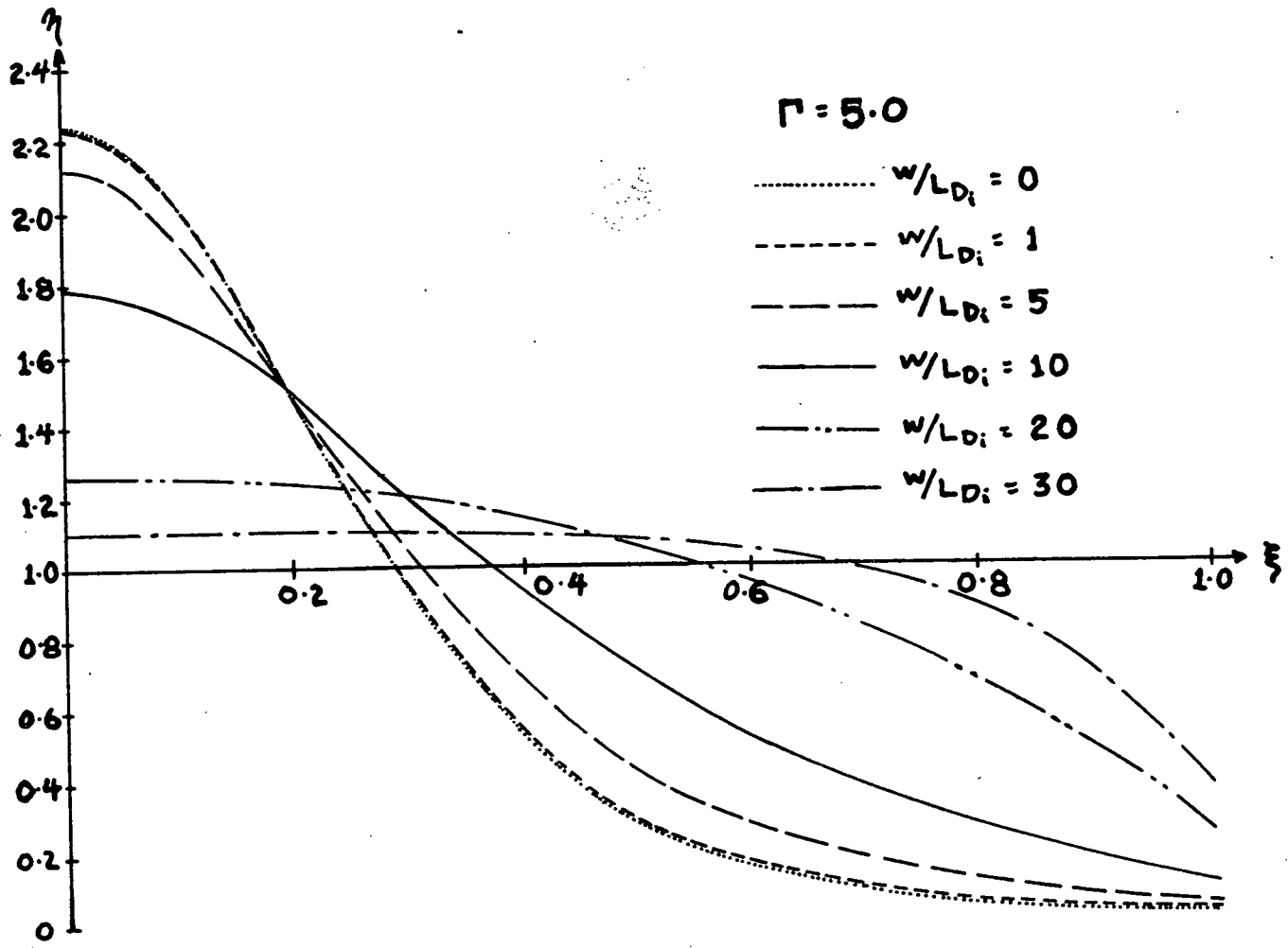


Figure 3-3. Carrier distribution for  $\Gamma = 5.0$ ; various values of  $w/LD_i$ .

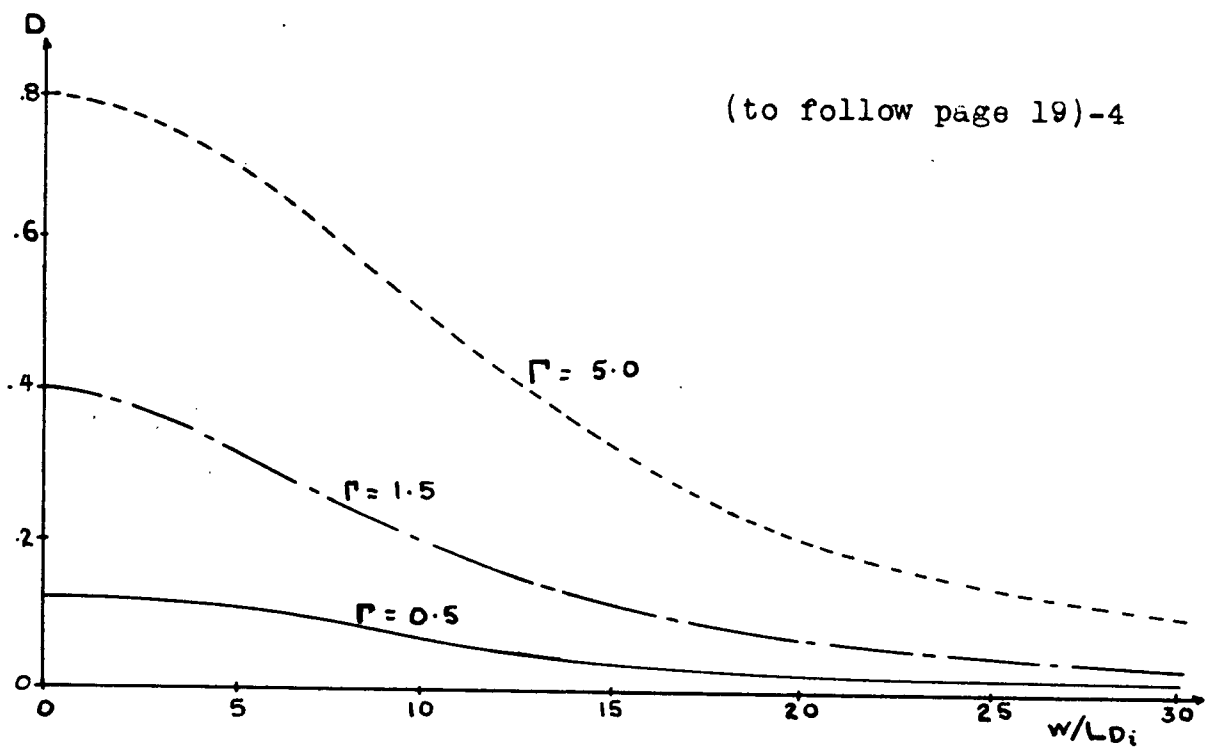


Figure 3-4a. Average absolute deviation of  $\eta$  from unity as a function of  $w/LD_i$  for three values of  $\Gamma$ .

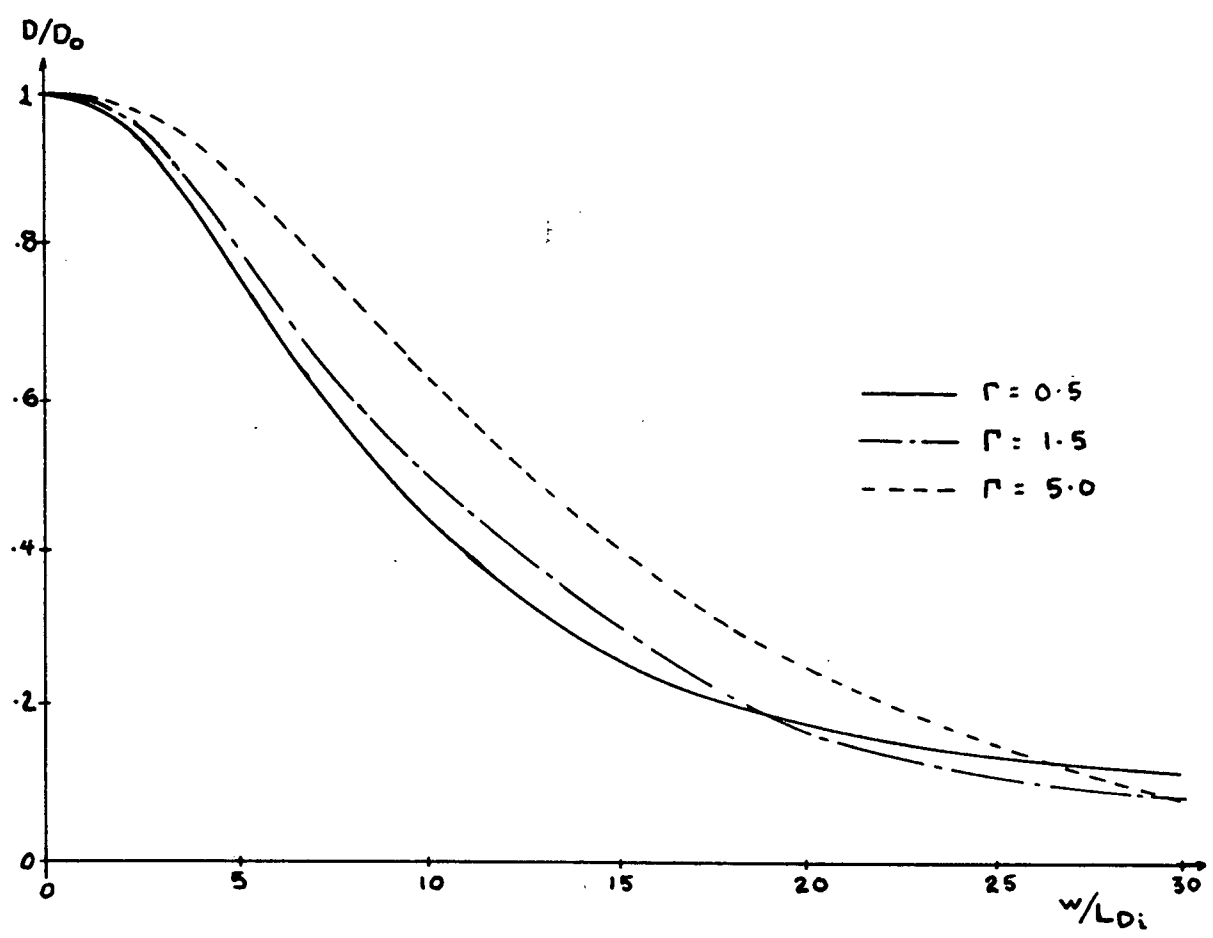


Figure 3-4b. Normalised average absolute deviation of  $\eta$  from unity as a function of  $w/LD_i$  for three values of  $\Gamma$ .

in intrinsic material, where  $B_s$  is a constant. In the case of the slab, we can take the major portion of the surface recombination into account merely by modifying the bulk recombination rate term,  $R_o$ , changing it to

$$R_o' = R_o + 2B_s n_i^2 / d \quad (3-13)$$

This does not account for generations at the edge of the slab, nor for the surface effects in a cylindrical sample. Since the generation rate will be increased considerably at the edge (or the surface of a cylinder), qualitatively it is obvious that the value of  $\eta(\pm 1)$  will be raised towards unity. Thus, with surface effects, one would expect the distribution of  $\eta$  in the  $x$ -direction to be, for the most part, as given by Figures 3-1, -2 and -3 except that near  $x=1$  one should expect  $\eta$  to rise sharply towards unity.

### 3.6 Recombination Time

For the purpose of estimating the recombination time, we assume that initially  $\eta$  is equal to the value it would take in the absence of G & R ( $\eta_o$ ) and eventually falls to unity. Neglecting diffusion and magnetic effects:

$$\frac{\partial \eta}{\partial t} = \frac{R_o}{n_i} (1 - \eta^2)$$

whose solution is

$$\eta = \frac{\eta_o \cosh(2R_o t/n_i) + \sinh(2R_o t/n_i)}{\eta_o \sinh(2R_o t/n_i) + \cosh(2R_o t/n_i)}$$

This yields an exponential decay only near the cross-over point where  $\eta = 1$ . However, the time required for  $|\eta - 1|$  to fall to  $|\eta_0 - 1| / e$  ranges from  $0.45\tau_i$  for  $\eta_0 = 5$  to  $1.5\tau_i$  for  $\eta_0 = 0$ , where  $\tau_i = \frac{2R_0}{n_i}$  is the carrier lifetime in the undisturbed sample. Thus,  $\tau_i$  is a reasonable estimate of the recombination time,  $\tau_r$ .

If we should find that  $\tau_r$  is of the same order of magnitude or smaller than  $\tau_p$ , the pinch time, we may assume that the pinch builds up to the degree suggested by the above numerical analysis somewhat more slowly than as indicated by  $\tau_p$  (due to the retarding effect of the G & R). On the other hand, if  $\tau_p \ll \tau_r$ , we could expect the pinch to build up to about the extent suggested by the analysis neglecting G & R in a time  $\tau_p$ , overshooting its final value. Then after a total time  $\tau_r$  it would fall to the final state indicated by the numerical analysis of this chapter.

## 4. THERMAL EFFECTS

### 4.1 Assumptions

The purpose in discussing thermal effects is two-fold: Thermal pinching gives rise to a carrier distribution (or rather conductivity distribution) of precisely the same form as magnetic self-pinching; and negative resistance due to thermal effects could conceivably give rise to instabilities which could mask the presence of magnetic pinch.

In intrinsic semiconductors, the conductivity is given, to a good approximation, by:

$$\sigma = \sigma_0 e^{-E_g(\frac{1}{T} - \frac{1}{T_0})/2k} \quad (4-1)$$

where  $\sigma$  is the conductivity at temperature  $T$ ,  $\sigma_0$  the conductivity at the ambient temperature  $T_0$ , and  $E_g$  is the energy gap of the semiconductor. In the special case where

$$|\theta| = |(T - T_0)| \ll T_0$$

we may write

$$\sigma = \sigma_0 e^{G\theta} \quad (4-2)$$

where  $G = E_g / 2k T_0^2$

For the major portion of this discussion, we will be concerned with the steady state conditions, in which case the heat transport equation is:

$$\nabla^2 \theta + \sigma E^2 / K = 0 \quad (4-3)$$

where  $K$  is the thermal conductivity of the sample and  $E$  is

the applied electric field. Substituting (4- 2) into (4- 3) we obtain

$$\nabla^2 \theta + (6_0 E^2 / \kappa) e^{G\theta} = 0 \quad (4- 4)$$

As a boundary condition, it will be assumed that the outer surface of the sample is maintained at the ambient temperature  $T_0$ , suggesting vigorous cooling of the sample.

#### 4.2 Cylindrical Geometry

In the case of a cylinder, equation (4- 4) may be written

$$\frac{1}{r} \frac{\partial}{\partial r} \left( r \frac{\partial \theta}{\partial r} \right) + (6_0 E^2 / \kappa) e^{G\theta} = 0 \quad (4- 5)$$

assuming purely radial heat flow.

With the boundary condition quoted in section 4.1, the double-valued solution to (4- 5) is

$$\theta(r) = - \frac{2}{G} \ln \left\{ \frac{1}{2} \left( [1 \mp (1 - \lambda/2)^{1/2}] + [1 \pm (1 - \lambda/2)^{1/2}] [r/a]^2 \right) \right\} \quad (4- 6)$$

$$\text{where } \lambda = 6_0 a^2 E^2 G / \kappa \quad (4- 7)$$

The upper sign is taken in (4- 6) for values of current above that at the turn-over field (where  $\lambda = \lambda_{\text{max.}} = 2.0$ ) and the lower sign for values of current below this value.

Thus, from (4- 6) and (4- 2),

$$\delta(r) = 4 6_0 \left\{ [1 \mp (1 - \lambda/2)^{1/2}] + [1 \pm (1 - \lambda/2)^{1/2}] [r/a]^2 \right\}^{-2} \quad (4- 8)$$

which, as can be seen by comparison with equation (2- 8) gives the same form of conductivity distribution as does magnetic pinch.

Negative resistance occurs if the current exceeds the turn-over value,

$$I_T^{cyl.} = 2\pi a (26.0 K/G)^{1/2}$$

at which the power is

$$P_T^{cyl.} = 4\pi \ell K/G$$

and the electric field is at its maximum possible value

$$E_T^{cyl.} = \frac{1}{a} (2K/6.6)^{1/2}$$

(4-9)

We should also consider the conditions under which

$$\delta(o) = 2\delta_0 \quad (4-10)$$

since this condition will give rise to a distribution of conductivity comparable to that expected in magnetic pinch. This condition (4-10) is met if the current, power and electric field reach or exceed the values

$$I_{cr}^{cyl.} (thermal) \approx 0.64 I_T^{cyl.}$$

$$P_{cr}^{cyl.} (thermal) \approx 0.59 P_T^{cyl.} \quad (4-11)$$

$$E_{cr}^{cyl.} (thermal) \approx 0.91 E_T^{cyl.}$$

#### 4.3 Slab Geometry

Consider a slab in which the axes are oriented as shown in Figure 2-1. If the inequality  $d \ll w$  holds as in section 2.3, we may safely assume that nearly all of the heat flow takes place in the  $z$ -direction (i.e. through the thickness of the sample). In this case, (4-4) may be written

$$\frac{\partial^2 \theta}{\partial z^2} + (6.0 E^2 / K) e^{G\theta} = 0 \quad (4-12)$$

The solution of (4-12) with the surfaces at  $z = \pm \frac{d}{2}$  held at the temperature  $T_0$  is given by

$$\theta(z) = \frac{2}{G} \ln \left\{ \frac{\operatorname{sech}(2Tz/d)}{\operatorname{sech}(T)} \right\} \quad (4-13)$$

where  $T$  is given by the solution of the transcendental equation

$$T \operatorname{sech}(T) = E (d^2 G / 8K)^{1/2} \quad (4-14)$$

Thus from (4-2) and (4-13),

$$\sigma(z) = \sigma_0 \frac{\operatorname{sech}^2(2Tz/d)}{\operatorname{sech}^2(T)} \quad (4-15)$$

which again gives the same form of conductivity distribution as does magnetic pinch. (c.f. equation (2-21))

Negative resistance occurs if the current exceeds the turn-over value, as before:

$$I_T^{\text{slab}} \approx 3.02 w (26.0 K/G)^{1/2}$$

at which the power is

$$P_T^{\text{slab}} = 8 (w/d) \ell K/G \quad (4-16)$$

and the electric field is at its maximum value,

$$E_T^{\text{slab}} \approx \frac{1.32}{d} (2 K/6.0 G)^{1/2}$$

In the case of the slab, since the thermal pinching takes place in the thickness, and magnetic pinching is most pronounced in the width direction, as far as the measured conductivity distribution is concerned, the two forms of pinch are orthogonal and should not appreciably interfere with each other.

#### 4.4 Comparison of the Two Geometries

In order that the comparison between the cylinder be compatible with the comparison given in the case of magnetic pinch (section 2.4), we will again assume that the cross sectional area of the sample, and its length are kept the same in each case. The appropriate comparisons are between the turn-over current, power and field for the slab and the critical current, etc. for the cylinder:

$$\left. \begin{aligned} I_{CR}^{cyl. (thermal)} / I_T^{slab (thermal)} &= 1.35 (a/w) \\ P_{CR}^{cyl. (thermal)} / P_T^{slab (thermal)} &= 0.93 (d/w) \\ E_{CR}^{cyl. (thermal)} / E_T^{slab (thermal)} &= 0.69 (d/a) \end{aligned} \right\} (4-17)$$

#### 4.5 Heating in a Cylindrical Magnetic Pinch

We should consider the interaction between the magnetic and thermal pinch in detail, but to do so exactly complicates the equations involved. We can look at the effect magnetic pinch would have on the temperature distribution if the temperature dependence of the conductance is negligible. Let us assume that, in the case of the cylinder, the conductivity is given by

$$\sigma(r) = \sigma_i (1+ba^2) / (1+br^2)^2$$

from section 2.2 where  $\sigma_i$  is the initial conductivity and  $\sigma$  is

as defined in section 2.2. Equation (4-3) now becomes

$$\frac{1}{r} \frac{\partial}{\partial r} \left( r \frac{\partial \theta}{\partial r} \right) + (\delta_i E^2 / K) \frac{1 + ba^2}{(1 + br^2)^2} = 0$$

which yields upon integration

$$\theta(r) = (\delta_i E^2 / K) \frac{1 + ba^2}{4b} \ln \left\{ \frac{1 + ba^2}{1 + br^2} \right\}$$

which has the same radial dependence as that found in section 4.2. Thus, without considering increased magnetic pinching, we would expect the conductivity distribution to be enhanced by a factor

$$\approx \left[ \frac{1 + ba^2}{1 + br^2} \right] \left( \delta_i a^2 E^2 E_0 / 8k T_0^2 K \right)$$

for moderate or large  $b$ . Thus for the interaction of thermal and magnetic pinch to be negligible,

$$\frac{\delta_i a^2 E^2 E_0}{8k T_0^2 K} \ll 1 \quad (4-18)$$

i.e.  $E \ll E_T^{crit}$  of equation (4-9)

Of course, the above analysis only serves to give us a warning to look carefully for thermal effects in any pinch investigation, since magnetic and thermal pinch enhance each other.

## 5. PUBLISHED EXPERIMENTAL DATA

### 5.1 General Review

The first report claiming observance of magnetic self-pinching in a semiconductor was by Glicksman and Steele (1959). This was based upon a comparison of the current-voltage characteristics of an n-type indium antimonide (InSb) sample in the presence of a longitudinal magnetic field of varying strength. It was observed that in the absence of a magnetic field, the slope of the I-V curve was slightly smaller (in the avalanche breakdown region) than with a longitudinal field present. Since the value of current at which the curve without a magnetic field departs from that with the field is a not unreasonable estimate of  $I_{CR}$  (given in section 2.2) and since it is well known that a longitudinal magnetic field tends to inhibit pinch in a gaseous plasma, the observed phenomenon is ascribed to pinch. The reason given for the increased resistance under pinch conditions is that the current carriers are compressed into a smaller cross-section than the geometrical one, "...hence increasing the apparent resistivity".

In a more recent paper (Glicksman and Powlus, 1961) further attempts are made to corroborate the observance of pinch in n-type InSb. In this case, the temporal behaviour of the voltage across the sample is observed when a constant current pulse is passed through it. It is assumed that the electric field throughout the entire length of the sample

remains homogeneous, and is simply equal to the voltage across the sample divided by its length.

Initially the voltage across the sample was observed to rise to a very high value (corresponding to an electric field greater than  $3 \times 10^4$  V. m.<sup>-1</sup>). The voltage dropped (after about 0.04 microsecond) to a value corresponding to about  $2 \times 10^4$  V.m.<sup>-1</sup>. After an interval of time, denoted by  $t_2$ , the voltage again rose very slightly to a value at which it remained, aside from very slight fluctuations, until the end of the pulse.

The above observations were interpreted as follows: The initial rise was to a value which would result if breakdown did not occur. The drop was to the value required to sustain the breakdown condition, and the slight rise after a time  $t_2$  was ascribed to the establishment of a magnetic pinching of the hole-electron plasma created by breakdown.

The reciprocal of  $t_2$  was plotted against the plasma current (which was defined as the total current less the current due to the electrons originally present) and was compared to a theoretical relation:

$$1/t_{\text{pinch}} = (I - I_{\text{cr}}) / A \quad (5-1)$$

(Ancker-Johnson et al, 1961) where  $A = 2\pi a^2 / v_d \mu_r \mu$  where  $v_d$  is the electron drift velocity and  $\mu_r$  is "the radial mobility of the plasma", which would be approximately  $2\mu_p$  in this case.  $I_{\text{cr}}$  is of the same form as given in section 2.2. The comparison yielded reasonable values for  $\mu_p$  and  $k(T_n + T_p)$ .

Further work done at R.C.A. Laboratories (Ancker-Johnson, et al, 1961) involved virtually the same experiment as quoted above, except that p-type InSb was used. Also, the initial drop in voltage as described above was ascribed to injection of carriers rather than avalanching. (The oscillographs shown in this work are identical in form to those shown by Glicksman and Powlus.) Here again, the increased observed resistance was explained by: "...the cross-sectional area carrying the current was reduced from the geometrical cross-section to the pinch cross-section."

Chynoweth and Murray (1961) also put forth evidence of having observed pinch in n-type InSb. They used three different methods. The first was almost identical to that used by Glicksman and Steele (1959) described above, except that Chynoweth and Murray were careful to see that the critical current occurred well into the avalanche breakdown region. The critical current was observed to be about 4 amperes. They also derived the critical current by plotting the current at which "pinch" set in against magnetic field. This is compared to the well known theory of gaseous pinch (e.g. Linhart, 1961, p. 221 ):

$$I_{pinch} = I_{CR} + (B_z^2 / I_{pinch}) \cdot \left(\frac{a}{2}\right)^2$$

where  $I_{CR}$  is as given in section 2.2. The plot yielded a critical current of 4.4 amperes and gave a value of  $a$  in excellent agreement with the actual radius of the sample.

The third method used involved a similar experimental arrangement as that of Glicksman and Powlus (1961) described above. However the observations were quite different. The sample was subjected to constant current pulses. Below  $I_{cr}$  the voltage remained constant throughout the pulse, and well above  $I_{cr}$  the voltage remained constant at a slightly higher value. In the neighborhood of  $I_{cr}$  the voltage fluctuated between that when  $I < I_{cr}$  and that when  $I > I_{cr}$ . The value of current at which these fluctuations were the most pronounced was taken to be  $I_{cr}$ . ( $I_{cr} \approx 4$  to 6 amp.)

In this work, three separate methods of obtaining  $I_{cr}$  gave good agreement. Chynoweth and Murray ascribe the increased resistance of the pinched plasma to the combined effects of hole-electron scattering which is increased due to the higher concentration of carriers near the center of the sample, and to a lesser extent increased magneto-resistance. They state that these changes cannot account for a change in resistance as large as was observed, at least not according to present theory. The fluctuations observed when  $I \approx I_{cr}$  were explained by a pinching-unpinching instability. No instability in the "pinched" condition was observed.

## 5.2 Critical Summary

Probably the most disturbing feature of the above reports of observance of magnetic self-pinching is that all the arguments are based on an observed apparent change of resistance of the sample between the "pinched" and "unpinched"

states. It is particularly disturbing to see this change in resistance dismissed so glibly as is done by Glicksman and Steele and Ancker-Johnson et al (see section 5.1). Because the carriers are confined to travel in a smaller cross-section of the sample is no reason for the overall resistance to change in any way whatsoever, if the number of carriers and their mobilities remain the same. In magnetic pinching, any resistance change will be a purely secondary effect, such as that suggested by Chynoweth and Murray. We can dismiss the effect of magneto-resistance on the change in resistance as follows. Using the small field approximation for transverse magneto-resistance

$$\Delta R/R_0 = -\Delta \delta/\delta_0 \approx 10 B^2 \quad (5-2)$$

where the factor  $10 \text{ m.}^4 \text{ weber}^{-2}$  has been taken from the measurements of Frederikse and Hosler (1957). The above relation was derived for the change of resistance in a sample with a uniform conductivity and applied transverse magnetic field. We will, without further justification, assume that

$$\Delta R/R \approx 10 (2/\delta_i a^2) \int_0^a \delta B^2 r dr \quad (5-3)$$

If  $\delta$  and  $B$  are as given in section 2.2, in terms of

$$\eta_{(0)} = n^{(0)} / n_i \quad ,$$

$$\frac{\Delta R}{R} = 10 \left( \frac{\mu I}{2\pi a} \right)^2 \cdot \frac{2}{3} \cdot \frac{(\eta_{(0)} + 2)(\eta_{(0)} - 1)^2}{\eta_{(0)}} \quad (5-4)$$

whereas if the current density were homogeneous we would have

$$\frac{\Delta R}{R} = 10 \cdot \frac{1}{2} \left( \frac{\mu I}{2\pi a} \right)^2 \quad (5-5)$$

With no G & R at the critical current ( $I_{(0)} = 2$ ) of 4 amperes and sample radius of  $2.5 \times 10^{-4}$  m. (Chynoweth and Murray, 1961) (5-4) gives

$$\Delta R / R \approx 13 \times 10^{-5}$$

and (5-3) gives  $\Delta R / R \approx 5 \times 10^{-5}$

Thus the effect of magneto-resistance on the total resistance of the sample is negligible, even during pinch.

It is rather difficult to comment on the form of time dependence of the pinch obtained by Glicksman and Powlus since their theory is unpublished. However, if we look at equation (2-28) we see that initially

$$\left( \frac{\partial g}{\partial t} \right)_{t=0} = - \frac{\mu_n \mu_p}{\mu_n + \mu_p} \cdot \frac{\mu I^2}{4\pi^2 a^2} \quad (5-6)$$

If the plasma were to contract at this rate until  $g = 0$ , we would get the following expression for the pinch time:

$$\frac{1}{t_{\text{pinch}}} = \frac{\mu_n \mu_p}{\mu_n + \mu_p} \cdot (v_n + v_p) \cdot \frac{\mu I}{2\pi a^2} \quad (5-7)$$

(c.f. Ancker-Johnson's  $1/(\mu_r v \mu / 2\pi a^2)$  as given in the previous section;  $v_n \gg v_p$  so if  $\mu_r \approx 2\mu_n \mu_p / (\mu_n + \mu_p)$ ,  $1/A$  is identical to the factor we have multiplying  $I$ ). This is still not quite the same form as given by Glicksman. However, if he assumes that no pinching occurs at  $I \leq I_{cr}$ , then for  $\partial g / \partial t \leq 0$  under these conditions, he would have to replace  $I$  by  $(I - I_{cr})$  in equation (5-7), which then gives the form quoted by Ancker-Johnson et al. In the above, the effects of diffusion have

been completely ignored. Using the values for the properties of InSb at 77°K. quoted by Glicksman and Powlus (1961),  $1/A \approx 3 \times 10^6 \text{ coul.}^{-1}$ , giving

$$\frac{1}{t_{\text{pinch}}} \approx 3 \times 10^6 (I - I_{cR}) \text{ sec.}^{-1}$$

Our estimate of  $1/\tau_p$  from equation (2-31) gives values ranging from  $2.5 \times 10^6 \text{ sec.}^{-1}$  for very weak pinching to  $0.85 \times 10^6 \text{ sec.}^{-1}$  for very strong pinching. Both methods yield about the same size of pinch time, but completely different current dependence.

Another disturbing feature of the above work is that all of it was done under avalanche breakdown conditions, under which the theory of the behaviour of semiconductors is still rather uncertain. These conditions will tend to produce non-uniform plasma densities. The possibility that the observations made by the above workers are due to as yet unexplained behaviour of semiconductors under avalanche conditions, or to injection effects, cannot be completely ruled out. In particular, space charge instabilities (not involving magnetic effects) merit attention as possible mechanisms.

There would not be so great an objection to operating the samples in the avalanche region if the experiments were designed in such a way that the results could unambiguously tell whether pinch were present or not. Measurements were of effects of secondary importance: change of resistance and time dependent responses which could conceivably be caused

by some other mechanism than pinch. During the avalanche process, the longitudinal electric field and the ratio of  $\bar{J}_n / \bar{J}_p$  are inhomogeneous in the longitudinal direction. Hence we have effectively a plasma whose properties vary along its length and in time. All derivations of pinch theory assume that the properties of the plasma are uniform longitudinally and require  $(J_{n3} / J_{p3})$  to be constant and equal to  $\mu_n / \mu_p$ . Hence a plasma generated by avalanche gives an unsatisfactory medium for a rigorous comparison of theory to experimental results. Anomalous effects are also likely to occur under these conditions and hence only circumstantial and inconclusive evidence of pinch is available.

## 6. EXPERIMENTAL CONSIDERATIONS

### 6.1 Observable Characteristic of Pinch

We have seen that the overall resistance changes which might occur during the self-pinching are only of secondary importance. The main characteristic of pinch is a change in the distribution of the carriers, accompanied by a corresponding change in the conductivity distribution. The only type of experiment which can unambiguously determine whether or not pinching is present is one which gives us an indication of the carrier distribution in the sample. We will consider a few possible schemes for observing this redistribution of conductivity and then try to suggest a possible experimental approach to follow.

## 6.2 Radio-Frequency Measurements

Let us consider the application of a high-frequency magnetic field to the sample by means of a coaxial solenoid. We will make the following simplifying assumptions:

- a) In the absence of the sample, the magnetic field is homogeneous and of the same phase throughout.
- b) Between the sample (radius  $a$ ) and the solenoid (radius  $r_0$ ), the magnetic field is the same as if the sample were not present.
- c) The skin depth,  $\delta = (2/\mu\sigma\omega)^{1/2} \ll a$ .  $\omega$  is the angular frequency of the r.f. test signal.
- d)  $\epsilon\omega \ll \sigma$  so that displacement currents are negligible.

When the above hold, we get from Maxwell's equations and the boundary conditions, for small changes in conductivity within the skin depth

$$\Delta Z(\omega) \approx -\frac{1}{2} \left(\frac{a}{r_0}\right)^2 \frac{\delta}{a} \omega L_0 (1+j) \frac{\Delta\sigma}{\sigma}$$

where  $L_0$  is the inductance of the solenoid in the absence of the sample. While the above is only valid for relatively small changes in conductivity at the outer edge, if the carrier distribution is a monotonically decreasing function of the radius (as is the case if there is no surface G & R) the apparent inductance will be an increasing function of the strength of the pinch. For greatest sensitivity, the

radius of the sample should be as close to the radius of the solenoid as possible.

An alternative method of using r.f. techniques to obtain an estimate of carrier redistribution is to measure the impedance seen by a longitudinal r.f. electric field. We retain assumptions c) and d) above.

$$\Delta Z(\omega) \approx - \frac{\ell}{2\pi a} (2\mu\omega/\sigma)^{1/2} (1+j) \frac{\Delta\sigma}{\sigma_0}$$

for small changes in conductivity within the skin depth.

One of the most important assumptions used in the above analysis is that  $\delta \ll a$ . This condition must be met in order that changes in the distribution will be measureable.

We can find the size of  $\omega$  required to meet this condition for two semiconductors whose properties are given in the appendix.

$$\text{InSb at } 160^\circ\text{K. : } \omega \gg 8 \times 10^5 / \text{ sec.}^{-1}$$

$$\text{Ge at } 300^\circ\text{K. : } \omega \gg 5 \times 10^3 / \text{ sec.}^{-1}$$

where  $a$  is measured in meters. For other considerations we will see that we should not allow  $a$  to be much greater than  $10^{-3}$  m. Hence the frequency which would be required is well into the kilomegacycle region.

There are two important drawbacks to the use of microwave measurements. The first is that any changes in overall resistance would have to be carefully considered. The other is that this method does not actually measure the conductivity distribution, but only gives an indication of

the changes which occur near the outer surface. Hence any surface G & R will tend to mask the changes which take place further into the sample.

### 6.3 Probe Techniques

Probes to measure the change in conductivity distribution could be applied to either the slab or cylinder. In the case of the cylinder, however, only an indication of the changes in the distribution would be obtained. As with the r.f. methods, the effects of surface G & R would tend to mask any internal changes. In the case of the slab one would actually measure the conductivity distribution by means of an a.c. test signal applied to pairs of probes attached to opposite faces of the slab at various distances from the longitudinal axis. In this arrangement the edge effects will in no way hide the internal carrier redistribution.

### 6.4 Infrared Absorption

Harrick (1956) has described a method by which the absorption of infrared by the free carriers in a semiconductor may be used to determine their distribution. The experimental arrangement is shown schematically in Figure 6-1. For each position of the slit and detector on the sample, the transmitted intensity  $I_t$  would be measured without any current passing through the sample. This would then be balanced out by a bridge circuit. The current would then

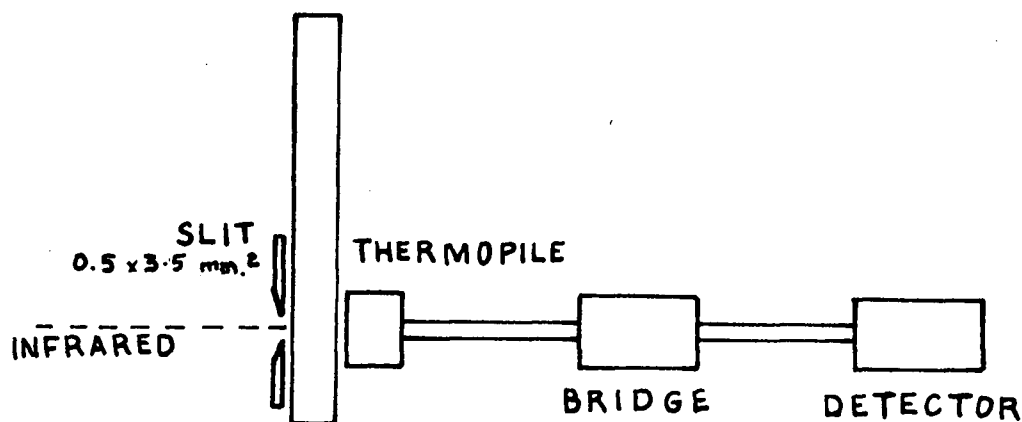


Figure 6-1. Experimental arrangement for measuring the carrier distribution by infrared absorption.

be applied to the sample, and  $\Delta I$ , the change in transmitted intensity would be measured. The carrier distribution could then be found through the relation given by Harrick:

$$\Delta I / I_T \approx (e^{c(n-n_0)d} - 1)$$

where  $c$  is a constant and  $d$  is the thickness of the sample. On the basis of Harrick's measurements on a sample about 1 cm. thick, one should be able to detect changes in carrier concentration of about  $10^{19} \text{ m.}^{-3}$  in a slab 0.5 mm. thick. This would adequately demonstrate pinch if it were to occur.

It should be noted that it takes about one second to make a measurement, the time constant of the thermopile. Thus if pinch in semiconductors turns out to be a short-lived phenomenon as it is in gaseous plasmas, this method would not detect it.

### 6.5 Generation of a Hole-Electron Plasma

We will consider four methods of generating a hole-electron plasma: avalanche breakdown, injection, thermal generation, and photo-ionization.

The major objection to using avalanche breakdown has been outlined in section 5.2. It is a stochastic cascade process which is not fully understood. Even though pinching might occur in a plasma generated in this way, one cannot be certain that other phenomena (e.g. space charge effects) would not interfere with the observations.

Injection would lead to a non-uniform longitudinal carrier distribution, especially in an intrinsic semiconductor. In addition, the dependence of carrier injection on the type of contact and the carrier density is not yet fully understood. It does not seem advisable to search for a specific phenomenon in a plasma generated by a method which is likely to give rise to unknown effects.

Probably the best understood method of creating a hole electron plasma is by thermal generation. For this method, the sample used should have as low an impurity concentration as may be obtained practically. We can readily estimate the magnitude of pinch even with G & R in this case, which is not true in the previously mentioned situations.

Photo-ionization is predominantly a surface effect unless the radiation is filtered by a slab of the same semiconductor in order to pass only those photons with good penetration. If we consider the effect of shining properly

filtered light uniformly on both faces of a slab, we can approximate the photo-ionization by a constant pair generation rate throughout the sample,  $R_s$  m.<sup>-3</sup> sec.<sup>-1</sup>. Taking the  $x$ -component, equation (3- 3) becomes:

$$\frac{\partial J'_x}{\partial x} = q [R_s + R_o (1 - [n/n_i]^2)] = q R' (1 - \eta'^2)$$

where  $R' = R_o + R_s$  and  $\eta' = \frac{n}{n_i} [1 + \frac{R_s}{R_o}]^{1/2}$

The net effect of this is to raise the values of  $n_i$ ,  $(w/L_o)^2$  and  $\Gamma$  by a factor of  $(1 + R_s/R_o)^{1/2}$  in equation (3- 5). The situation is then essentially unchanged from purely thermal generation except that the effective  $n_i$  is increased.

From the above considerations, it would seem that the best method of producing a plasma for the study of self-pinching would be thermal generation. With this method spurious effects are less likely to interfere with the observations of pinch.

## 6.6 Geometry and Material

Having decided upon the means of generating the plasma, we should now consider the geometry of the sample. In the case of the slab, we can measure the carrier distribution whereas with the cylinder we can obtain only a rough estimate of the way in which this distribution changes. From this consideration, if all else were equal, it would seem that the slab geometry is superior.

We should now compare the slab and cylinder from the consideration of minimizing thermal effects. To do this, we compare the ratios of minimum power required to initiate self-pinching to the maximum power permitted without thermal effects becoming important for the two geometries. From equations (2-20) and (4-17)

$$\frac{P_{CR}^{slab}(\text{pinch}) / P_T^{slab}(\text{thermal})}{P_{CR}^{cyl}(\text{pinch}) / P_{CR}^{cyl}(\text{thermal})} = 1.69 (d/w)^2 \quad (6-1)$$

Since  $d \ll w$  it is apparent that the slab is superior from this consideration. Since we require the critical electric field (for magnetic pinching) to be below the breakdown field, the slab is again superior.

Recall equation (2-20):  $E_{CR}(\text{slab}) / E_{CR}(\text{cyl.}) = (2d/\pi w)^{1/2}$

We should now consider the problem of surface G & R. We do not expect the bulk G & R to give appreciably different results in the two geometries. Because the slab has a much greater surface area for its volume than the cylinder, we might expect surface G & R to present a greater problem in the slab. However, here the main effect of surface G & R is to increase the effective bulk recombination rate. In addition a small increase of carrier concentration will result at the edges. The primary effect in the cylinder will be to increase the carrier concentration at the outer surface. This

increase could mask the measurement of the internal changes in carrier density, as we have pointed out in the preceding sections.

Thus, it appears that the slab geometry is superior from all considerations.

We must now consider the material to be used in any experiment designed to observe self-pinching. In the appendix, we have listed a number of properties of three representative semiconductors: Silicon (Si), Germanium (Ge), and Indium Antimonide (InSb).

From equations (2-19) and (4-16) we get

$$\frac{P_{CR} \text{ (pinch)}}{P_T \text{ (thermal)}} \approx \frac{E_g}{\mu q (\mu_n + \mu_p) T K} \cdot \left(\frac{d}{w}\right)^2 \quad (6-2)$$

where we have assumed that  $T_n \approx T_p \approx T$ , the ambient temperature. This is a slightly increasing function of temperature. The minimum temperature at which we could consider operating the sample would be the one at which the carrier density is about one order of magnitude greater than the impurity concentration. The practical minimum impurity concentration obtainable at the present time is about  $10^{19} \text{ m.}^{-3}$ . Thus we will denote the temperature which gives us a carrier concentration of  $10^{20} \text{ m.}^{-3}$  as  $T_{\text{min}}$ , our minimum operating temperature for a given sample. We will take the temperature at which the electron gas becomes degenerate as an upper

limit,  $T_{max}$ . From numerical values quoted in the appendix we have estimated and tabulated  $T_{min}$ ,  $T_{max}$ ,  $\frac{P_{CR}(\text{pinch})}{P_T(\text{thermal})} (T_{min})$ ,  $E_{CR}/E_b (T_{min})$ ,  $\tau_p (T_{min})$ ,  $\tau_r (= \tau_{i,max})$ , and  $\tau_{thermal} = \frac{C_p (d)}{K (z)}^2$  in table 6-1.  $E_b$  is the breakdown electric field.

TABLE 6-1			
	Silicon	germanium	indium antimonide
$T_{min} (^\circ K)$	400	310	160
$T_{max} (^\circ K)$	620	555	285
$\frac{P_{CR}(\text{pinch})}{P_T(\text{thermal})}$	$360(d/w)^2$	$60(d/w)^2$	$0.93(d/w)^2$
$E_{CR}/E_b$	$0.8 \times 10^{-3}/w$	$0.32 \times 10^{-3}/w$	$1.3 \times 10^{-3}/w$
$\tau_p (\text{sec.})$	$100 w^2$	$13 w^2$	$4.5 w^2$
$\tau_r (\text{sec.})$	$10^{-3}$	$10^{-3}$	$10^{-7}$
$\tau_{thermal} (\text{sec.})$	$5.8 \times 10^3 d^2$	$7.3 \times 10^3 d^2$	$2.5 \times 10^3 d^2$
Note: $d$ and $w$ are measured in meters			

Since  $w$ , the width of the slab can be made greater than  $2 \times 10^{-3}$  meters without any difficulty, there will be no problem in keeping below the breakdown field in any of these materials.

From  $P_{CR}(\text{pinch})/P_{CR}(\text{thermal})$ , which must be kept less than

unity to reduce thermal effects, we obtain a limit on  $d/w$ :

$$\text{Si: } d/w < .05$$

$$\text{Ge: } d/w < .13$$

$$\text{InSb: } d/w < 1.04$$

The above does not consider the interaction between thermal and magnetic effects nor the effects of G & R. Hence we should consider these limits on  $d/w$  as absolute maxima. In practice it would be difficult to obtain a ratio of much less than .05 so we can rule out the use of silicon at once.

We shall now look at the effect of G & R in germanium and indium antimonide. From the definition of  $L_D$ ; given in equation (3-4) and the numerical values given in the appendix:

$$L_{D_i}(\text{Ge}) \approx 1.8 \times 10^{-3} \text{ m.}$$

$$L_{D_i}(\text{InSb}) \approx 2.1 \times 10^{-5} \text{ m.}$$

The sample would likely have a width of about 1 cm., in which case

$$\text{Ge: } w/L_{D_i} \approx 5.5$$

$$\text{InSb: } w/L_{D_i} \approx 480$$

From chapter 3 we see that the G & R will completely dominate in the case of InSb without even considering the effect of surface recombination. Thus germanium looks as if it would be the most suitable material.

### 6.7 Summary

In this section we shall try to outline a possible experiment to be performed to observe self-pinching. For the sake of a numerical example, let us assume that we have a well-etched slab of highly pure germanium of cross-section 0.5 mm. x 1.0 cm. If the recombination velocity is 1 m./sec., we find that:

$$w/L_{D_i} \approx 12.5$$

This value is not too high: from the curves shown in chapter 3, we estimate that with  $\Gamma \approx 2 \rightarrow 3$  one should obtain a measurable pinch. This means a current of about

$$I \approx \left( 3 \times 16 k T n_i d^2 / \mu \right)^{1/2} \approx 1.5 \text{ amp.}$$

From table 6-1 we have

$$\tau_p \approx 1.3 \times 10^{-3} \text{ sec.}$$

$$\tau_r \approx 1.0 \times 10^{-3} \text{ sec.}$$

$$\tau_{\text{thermal}} \approx 1.8 \times 10^{-3} \text{ sec.}$$

Thus all the times involved are of the same order of magnitude. This means that we will have to take special care to reduce thermal effects, since any of these which occur will do so about the same time as pinching takes place. Since  $\tau_p \approx \tau_r$  we will expect the pinch to develop to the value calculated with G & R without any appreciable overshoot.

Some means of cooling the surface would have to be employed, since about 600 watts per cm. length of the sample would be dissipated. If pulses of current are used, these must be at least an order of magnitude longer than the characteristic times involved, i.e. at least  $10^{-2}$  sec.

It is proposed that initially the probe method (see sec. 6.3) should be employed to measure the carrier redistribution. If it should turn out that the pinch is stable for up to a second, the infrared absorption technique described in section 6.4 might be used.

## 7. CONCLUSIONS

In the above analysis we have shown that in order to make a rigorous comparison between any experiment designed to observe self-pinching and the theory at its present stage of development, we must use a thermally generated plasma, possibly enhanced by illumination with properly filtered light. The only unambiguous indication of self-pinching is the transverse redistribution of the carriers and hence the conductivity. Even this indication is subject to interference from thermal effects, which must be carefully accounted for in any experimental arrangement.

Finally, we have shown that if self-pinching can

occur in semiconductors, one should be able to observe it in a thermally generated plasma in a pure germanium slab at room temperature. Hence it is completely unnecessary to consider using the highly unsatisfactory avalanche-generated plasma for pinch studies, as has been done to date.

## APPENDIX

Some Properties of Three Intrinsic Semiconducting Materials:  
Silicon, Germanium and Indium Antimonide

## a) Silicon

Property	Value	Source of Information
$n_i$	$3.88 \times 10^{22} T^{3/2} e^{-0.605/kT} m^{-3}$ (kT in ev.)	Smith (1959)
$\mu_n$	$0.15(300/T)^{2.6} m^2/V.sec.$	Smith (1959)
$\mu_p$	$0.05(300/T)^{2.3} m^2/V.sec.$	Smith (1959)
$K(300^\circ K)$	84 watts/m. deg.	Smith (1959)
$C_p(300^\circ K)$	$1.64 \times 10^6 J./m.^3 deg.$	Smith (1959)
$\tau_i max.$	$10^{-3} sec.$	Smith (1959)
$E_g$	1.21 ev.	Smith (1959)
$T_{degen.}$	620° K.	Smith (1959)
$E_b$	$2 \times 10^7 V./m.$	Chynoweth (1958)
$S_{min.}$	10 m/sec.	Jonscher (1960)

## b) Germanium

Property	Value	Source of Information
$n_i$	$1.76 \times 10^{22} T^{3/2} e^{-.3925/kT} m^{-3}$	Smith (1959)
$\mu_n$	$0.38(300/T)^{1.66} m^2/V.sec$	Smith (1959)
$\mu_p$	$0.18(300/T)^{2.33} m^2/V.sec.$	Smith (1959)
$K(300^\circ K)$	63 watts /m. deg.	Smith (1959)
$C_p(300^\circ K)$	$1.85 \times 10^6 J/m.^3 deg.$	Smith (1959)
		(over)

## Germanium (continued)

Property	Value	Source of Information
$\tau_{i \max}$	$10^{-3}$ sec.	Smith (1959)
$E_g$	0.785 ev.	Smith (1959)
$T_{\text{degen.}}$	$555^\circ$ K.	Smith (1959)
$E_b$	$8 \times 10^6$ V./m.	Smith (1959)
$S_{\text{min}}$	1 m/sec.	Jonscher (1960)

## c) Indium Antimonide

Property	Value	Source of Information
$n_i$	$1.29 \times 10^{22} (\tau/290)^{3/2} e^{-\frac{1215}{kT} (1 - \frac{T}{290})} \text{ m.}^{-3}$	Smith (1959)
$\mu_n$	$7.0 (300/\tau)^{1.68} \text{ m}^2/\text{V. sec.}$	Smith (1959)
$\mu_p$	$0.09 (300/\tau)^{2.1} \text{ m}^2/\text{V. sec.}$	Smith (1959)
$K(160^\circ\text{K})$	67 watts /m.deg.	Busch and Schneider, (1954)
$C_p(160^\circ\text{K})$	$0.665 \times 10^6 \text{ J/m}^3 \text{ deg.}$	Gul'tyaev and Petrov (1959)
$\tau_{i \max}$	$10^{-7}$ sec.	Smith (1959)
$E_g$	.255 ev.	Smith (1959)
$T_{\text{degen}}$	$285^\circ$ K.	Smith (1959)
$E_b$	$2 \times 10^4$ V./m.	Kanai (1959)

In the above, the symbols are defined as follows:

$n_i$  - undisturbed intrinsic carrier concentration

$\mu_n, \mu_p$  - electron and hole mobilities respectively

$K$  - thermal conductivity

$C_p$  - specific heat per unit volume

- $\tau_{i\max}$  - maximum practically obtainable carrier lifetime in the undisturbed sample.
- $E_g$  - energy gap (extrapolated to 0° K.)
- $T_{\text{degen}}$  - temperature at which the electron gas becomes degenerate.
- $E_b$  - electric field required to initiate avalanche breakdown.
- $S_{\text{min}}$  - minimum practically obtainable surface recombination velocity.

References for the Appendix:

- Busch, G. and Schneider, M., *Physica*, 20, 1084, (1954)
- Chynoweth, A. G., *Phys. Rev.* 109, 1537, (1958)
- Gul'tyaev, P. V. and Petrov, A. V., *Sov. Phys. Solid State*, 1, 330, (1959)
- Jonscher, A. K., Principles of Semiconductor Device Operation (John Wiley & Sons Inc., 1960)
- Kanai, Y. J. *Phys. Soc. Japan*, 14, 1302, (1959)
- Smith, R. A., Semiconductors, (Cambridge University Press, 1959)

## BIBLIOGRAPHY

- Ancker-Johnson, Betsy; Cohen, R. W.; and Glicksman, M.,  
Phys. Rev. 124, 1745 (1961)
- Bennett, W. H., Phys. Rev. 45, 891 (1934)
- Chynoweth, A. G. and Murray, A. A., Phys. Rev. 123, 515, (1961)
- Frederikse, H. P. R. and Hosler, W. R., Phys. Rev. 108, 1136  
(1957)
- Glicksman, M. and Steele, M.C., Phys. Rev. Letters, 2, 461  
(1959)
- Glicksman, M. and Powlus, R. A., Phys. Rev. 121, 1659, (1961)
- Harrick, N. J. Phys. Rev. 101, 491, (1956)
- Linhart, J. G. Plasma Physics, (North-Holland Publishing Co.,  
1961)
- Smith, R. A., Semiconductors, (Cambridge University Press,  
1959)